(12) INTERNATIONAL APPLICATION PUBLISHED UNDER THE PATENT COOPERATION TREATY (PCT)

(19) World Intellectual Property Organization
International Bureau

(43) International Publication Date
24 February 2022 (24.02.2022)

WIPO | PCT

(10) International Publication Number
WO 2022/040384 A1

(51) International Patent Classification:
H05B 33/14 (2006.01) *G02B 5/30* (2006.01)
G02B 1/00 (2006.01) *G02B 27/28* (2006.01)
G02B 5/00 (2006.01) *G02B 27/00* (2006.01)
G02B 5/18 (2006.01)

(21) International Application Number:
PCT/US2021/046622

(22) International Filing Date:
19 August 2021 (19.08.2021)

(25) Filing Language: English

(26) Publication Language: English

(30) Priority Data:
63/068,473 21 August 2020 (21.08.2020) US

(71) Applicant: **BOARD OF REGENTS, THE UNIVERSITY OF TEXAS SYSTEM** [US/US]; 210 West 7th Street, Austin, Texas 78701 (US).

(72) Inventors: **DODABALAPUR, Ananth**; 11 Sugar Shack Drive, West Lake Hills, Texas 78746 (US). **XU, Xin**; 7584 Chevy Chase Drive, Apt. 201, Austin, Texas 78752 (US). **KWON, Hoyeong**; 574 Jinju daero, Jinju si, Gyeongsan namdo, Gyeongsangnam-do 52823 (KR).

(74) Agent: **TIEFF, Michael** et al.; Meunier Carlin & Curfman LLC, 999 Peachtree Street NE, Suite 1300, Atlanta, Georgia 30309 (US).

(81) Designated States *(unless otherwise indicated, for every kind of national protection available)*: AE, AG, AL, AM, AO, AT, AU, AZ, BA, BB, BG, BH, BN, BR, BW, BY, BZ, CA, CH, CL, CN, CO, CR, CU, CZ, DE, DJ, DK, DM, DO, DZ, EC, EE, EG, ES, FI, GB, GD, GE, GH, GM, GT, HN, HR, HU, ID, IL, IN, IR, IS, IT, JO, JP, KE, KG, KH, KN, KP, KR, KW, KZ, LA, LC, LK, LR, LS, LU, LY, MA, MD, ME, MG, MK, MN, MW, MX, MY, MZ, NA, NG, NI, NO, NZ, OM, PA, PE, PG, PH, PL, PT, QA, RO, RS, RU, RW, SA, SC, SD, SE, SG, SK, SL, ST, SV, SY, TH, TJ, TM, TN, TR, TT, TZ, UA, UG, US, UZ, VC, VN, WS, ZA, ZM, ZW.

WO 2022/040384 A1

(54) Title: USE OF REFLECTING METASURFACES TO ENHANCE OUTCOUPLING ON ORGANIC LEDS AND OLED DISPLAYS

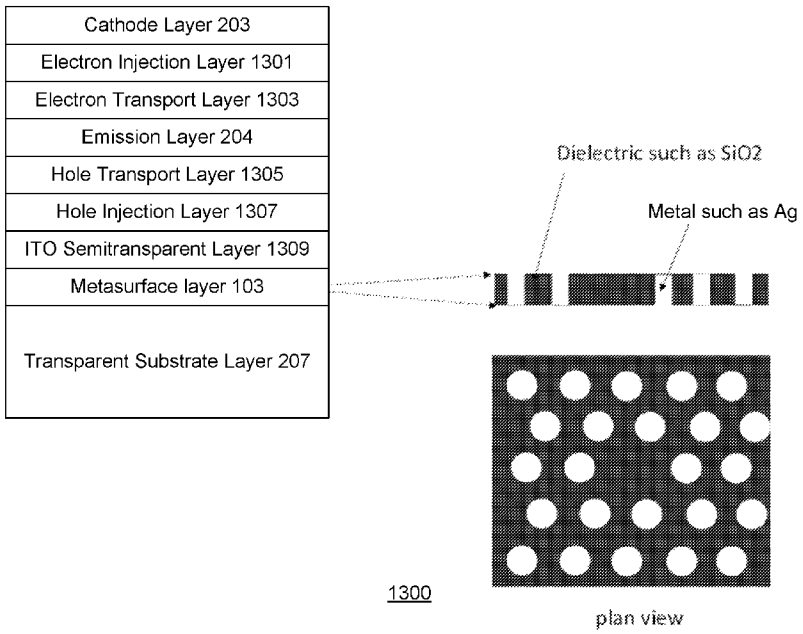

FIG.13

(57) Abstract: In an embodiment, a reflecting metasurface layer (103) is applied below device layers (204) of an OLED (301). Other device layers are then deposited on top of this reflecting metasurface. The reflecting metasurface layer may consist of a 2-dimensional or 1-dimensional pattern of two or more different materials. The materials may include gold and a transparent material with a refractive index that is greater than 1.5. These two materials may be patterned into sub-wavelength patterns or lattices including a square lattice, a triangular lattice, a 1-dimensional grating, and a quasicrystal pattern.

[Continued on next page]

(84) **Designated States** *(unless otherwise indicated, for every kind of regional protection available)*: ARIPO (BW, GH, GM, KE, LR, LS, MW, MZ, NA, RW, SD, SL, ST, SZ, TZ, UG, ZM, ZW), Eurasian (AM, AZ, BY, KG, KZ, RU, TJ, TM), European (AL, AT, BE, BG, CH, CY, CZ, DE, DK, EE, ES, FI, FR, GB, GR, HR, HU, IE, IS, IT, LT, LU, LV, MC, MK, MT, NL, NO, PL, PT, RO, RS, SE, SI, SK, SM, TR), OAPI (BF, BJ, CF, CG, CI, CM, GA, GN, GQ, GW, KM, ML, MR, NE, SN, TD, TG).

Published:

— *with international search report (Art. 21(3))*

USE OF REFLECTING METASURFACES TO ENHANCE OUTCOUPLING ON ORGANIC LEDS AND OLED DISPLAYS

CROSS-REFERENCE TO RELATED APPLICATIONS

[0001] This application claims priority to U.S. Provisional Application Serial No. 63/068,473, filed on August 21, 2020, and entitled "USE OF REFLECTING METASURFACES TO ENHANCE OUTCOUPLING ON ORGANIC LEDS AND OLED DISPLAYS." The contents of which are hereby incorporated by reference in their entirety.

BACKGROUND

[0002] One of the largest limiting factors in the efficiency of Organic Light Emitting Devices (OLEDs) is the total internal reflection of the generated light as it attempts to leave the device. A large portion of the light that is generated by an OLED does not actually emit out of the device because of plasmonic losses and total internal reflection due to the high refraction index of the OLED material and the low index of the outside environment.

[0003] It is with respect to these and other considerations that the various aspects and embodiments of the present disclosure are presented.

SUMMARY

[0004] In an embodiment, a reflecting metasurface layer is applied below device layers of an OLED. Other device layers are then deposited on top of this reflecting metasurface layer. The reflecting metasurface layer may consist of a 2-dimensional or 1-dimensional pattern of two or more different materials. The materials may include gold and a transparent material with a refractive index that is greater than 1.5. These two materials may be patterned into sub-wavelength patterns or lattices including a square lattice, a triangular lattice, a 1-dimensional grating, and a quasicrystal pattern.

[0005] In an embodiment, a metamaterial layer such as a metasurface layer is applied below an emissive layer of an OLED. In addition, a planar microcavity is formed in the OLED. The metasurface layer enhances a forward emission of a range of wavelengths whose emission along the plane of the layers is suppressed. The microcavity provides spectral purity by allowing a narrow range of wavelengths to be omitted.

[0006] In an embodiment, a display is provided. The display includes: a first device layer; a second device layer; and a reflecting metasurface. The reflecting metasurface may be applied between the first device layer and the second device layer.

[0007] Embodiments may include some or all of the following features. The display may be an organic light emitting device (OLED) display. The metasurface may be a one-dimensional pattern. The metasurface may be a two-dimensional pattern. The reflecting metasurface may include a first material and a second material. The first material may be gold and the second material may have a refractive index of at least 1.5. The first material and the second material may be patterned into sub-wavelength patterns. The first material and the second material may be lattices. The lattices may include square lattices, triangular lattices, 1-dimensional gratings, and quasicrystal patterns.

[0008] In an embodiment, a display is provided. The display includes: a first device layer; a second device layer; a microcavity; and a metamaterial layer. The metamaterial layer is applied between the first device layer and the second device layer and the microcavity is between the metamaterial layer and the second device layer.

[0009] Embodiments may have some or all of the following features. The first device layer may be an emissive layer. The metamaterial layer may be applied to the display before the emissive layer. The metamaterial may include a metallic plasmonic subwavelength material. The display may be an organic light emitting device (OLED) display. The metamaterial layer may include a metagrating. The metagrating may have a minimum feature size that is greater than

100 nm. The metagrating may be manufactured using photolithography. The metagrating may be manufactured using 193 nm deep photolithography. The microcavity may be a planar microcavity. The display may be incorporated into an augmented reality or a virtual reality headset.

[0010] This summary is provided to introduce a selection of concepts in a simplified form that are further described below in the detailed description. This summary is not intended to identify key features or essential features of the claimed subject matter, nor is it intended to be used to limit the scope of the claimed subject matter.

BRIEF DESCRIPTION OF THE DRAWINGS

[0011] The foregoing summary, as well as the following detailed description of illustrative embodiments, is better understood when read in conjunction with the appended drawings. For the purpose of illustrating the embodiments, there is shown in the drawings example constructions of the embodiments; however, the embodiments are not limited to the specific methods and instrumentalities disclosed. In the drawings:

[0012] FIG. 1 is an illustration of a 2-dimensional metasurface;

[0013] FIG. 2 is an illustration of an OLED with a metasurface;

[0014] FIG. 3 is an illustration of an OLED;

[0015] FIG. 4 is an illustration of an example metagrating pattern;

[0016] FIG. 5 is an illustration of another example metagrating pattern;

[0017] FIG. 6 is an illustration of a graph of surface-normal emission intensity improvements for an OLED with a metagrating layer, a graph of the angular dependence of intensity for an OLED with a metagrating layer, a graph of peak enhancement range values, and a graph of polarization values;

[0018] FIG. 7 is an illustration of a graph showing the response of a 2D quasicrystal metagrating layer, a graph showing the overlaid characteristics of a quasicrystal metagrating layer vs a non-metagrating layer, and a graph of polarization as a function of wavelength;

[0019] FIG. 8 is an illustration of the differences in emissions between an OLED with the metamaterial layer versus an OLED without the metamaterial layer;

[0020] FIG. 9 is an illustration of an example OLED with and without a metamaterial layer;

[0021] FIG. 10 is an illustration of an example pattern for a metamaterial layer;

[0022] FIG. 11 is an illustration of a graph showing improvements to forward emission due to a metamaterial layer; and a graph showing the polarization of a display with a metamaterial layer at various alignments;

[0023] FIG. 12 is an illustration of a device with both a metasurface layer and a microcavity;

[0024] FIG. 13 is an illustration of an example first structure; and

[0025] FIG. 14 is an illustration of an example second structure.

DETAILED DESCRIPTION

[0001] FIG. 1 is an illustration of a 2-dimensional metasurface 101. In some embodiments, the metasurface 101 may include a conducting backplane, a variable spacer, and a patterned metasurface. The metasurface 101 may include a metagrating layer 103 (also referred to herein as a metamaterial layer 103) with both quasiperiodic and periodic 2-dimensional patterns of metal and dielectric materials and a reflector layer 105. Other materials may be used.

[0002] FIG. 2 is an illustration of a top emitting organic light emitting diode (OLED) 201. As shown, the OLED 201 includes several layers including a cathode layer 203, an emission

layer 204, a reflector layer 205, and a substrate layer 207. More or fewer layers may be supported (e.g., the ETL, HBL, HTL, and TCO layers).

[0003] FIG. 3 is an illustration of an OLED 301 showing how the metagrating layer 103 of FIG. 1 can be incorporated into the OLED 201 of FIG. 2. As shown, the metagrating layer 103 is applied between the emission layer 204 and the reflector layer 205 of the OLED 301. By placing the metagrating layer 103 between the emission layer 204 and the reflector layer 205, the efficiency of the OLED is increased. The OLED 301 may further include transparent organic transporting (TCTA) layers and a ZrO_2 layer.

[0004] FIG. 4 is an illustration of an example metagrating pattern 401 that may be used for the metagrating layer 103 of FIG. 1. In the example shown, the metagrating layer 103 is a 2-dimensional square grating of gold cylinders. FIG. 5 is an illustration of another example metagrating pattern 501 that may be used for the metagrating layer. In the example shown, the metagrating layer is a quasicrystal pattern of gold cylinders with 5-fold symmetry.

[0005] In both of the metagrating layer patterns 401 and 501 the spaces between the cylinders may be filed with a solution deposited dielectric. A suitable dielectric is ZrO_2. Other dielectrics may be used.

[0006] In some embodiments, the patterning and integration of metasurfaces such as metagrating layers 103 into the light emitting device structures (e.g., OLED 301) is seamless and may be done before the sensitive organic layers are deposited. For example, the metagrating layer 103 may be applied before the emission layer is applied. This may allow for a more streamlined and efficient manufacturing process.

[0007] In some embodiments, the use of ZrO_2 (n = 1.7-2.0) as a dielectric layer is to mimic the optical properties of transparent conducting oxides, such as indium tin oxide, that are commonly used as anodes in OLEDs. TCTA, one of the materials used, is a commonly used charge transport layer in OLEDs. One level of high-resolution patterning may be necessary to define the

metal geometry of the metagrating layer. This may be performed using emerging scalable high-throughput nanomanufacturing techniques such as nanoimprint lithography. The features sizes used in the metasurfaces and metagratings are what can be conveniently realized by nanoimprint lithography.

[0008] The metamaterial enhanced OLED design described herein is independent of a substrate used and can be fabricated in a variety of ways that are suitable for a given substrate. For OLED displays on silicon substrates, the metamaterial pattern can be defined using UV photolithography commonly associated with silicon. For OLED displays on other substrates such as glass or plastic, nanoimprint lithography may be used for patterning and may also be used to define the metamaterial pattern. Other substrates and fabrication schemes will also be compatible if the metamaterial pattern can be defined properly.

[0009] In order to show the improvements to both intensity and polarization, a test OLED was constructed with light emission from a 50-nm thick layer of 8-hydroxyquinolonato aluminum and a metagrating layer as described above. The luminescence of the OLED was measured with a microscope/camera and a fiber-coupled spectrometer. The optical excitation is provided by a 405 nm laser. Other types of lasers may be used.

[0010] Surface normal emission was imaged with a camera though a monoscope with adjustable magnification. This arrangement allows accurate comparisons of intensities relative to non-metasurface devices and the use of statistical averaging of a large number of individual measurements to greatly improve accuracy of results. The use of a series of bandpass filters placed between the devices and the microscope transformed a broadband emitter into a series of relatively narrow-band emitters with 10 nm linewidth in the range 460 nm to 640 nm. In some measurements, polarization filters were also used to study the degree of polarization of emitted light.

[0011] FIG. 6 is an illustration of four graphs 601 (e.g., the graphs 601A-601D) of surface-normal emission intensity improvements for a 320 nm period square lattice metagrating layer for different spacer thicknesses. A 0% enhancement means that that the intensities of the non-metasurface and metasurface areas (both of which may have the same silver back-reflector) are the same, while a 100% enhancement means that the metasurface layer has twice the intensity.

[0012] As can be seen in the graph 601A, the maximum intensity enhancement of the metagrating layer achieved is 240% (or 3.4x) with a spacer layer thickness of 200 nm. The function of the spacer may be to control a number of diffraction channels that the emitted light can couple into. Generally, the thicker the spacer the fewer the diffraction channels and greater the peak enhancement of the metagrating layer. As shown, varying the thickness of the ZrO_2 spacer layer between 95nm and 200nm greatly changed the performance of the overall device. Note that the embodiments are not limited to ZrO_2 spacer layers of between 95nm and 200nm. It is contemplated that spacer layers of less than 95 nm, including zero, may be used.

[0013] The graph 601B shows the angular dependence of intensity. As can be seen, the normal direction intensity is enhanced by the metagrating layer 103 while the off-axis intensity drop-off is not too steep after the initial sharp decline. The enhanced intensity in the normal direction is compensated by reduced propagation in the in-plane direction. In a square metasurface, the wavelength range for peak enhancement corresponds to the periodicity of the metasurface.

[0014] The graph 601C shows how peak enhancement range varies when changing the period from 320 to 290 nm. The graph 601D shows how polarization improves for different wavelength and alignment. The degree of polarization depends on the wavelength with the maximum polarization anisotropy occurring when the intensity enhancement is the greatest.

[0015] FIG. 7 is an illustration of three graphs 701 (e.g., the graphs 701A-701C) showing various properties of the metagrating layer 103. The graph 701A shows the response of a 2D quasicrystal metagrating layer. The degree of intensity enhancement in quasicrystal metagrating layers 103 is less than in periodic metagrating layers but occurs over a broader range of wavelengths. Importantly, the angular dependence of emission intensity falls off very slowly.

[0016] The graph 701B shows the overlaid characteristics of a quasicrystal metagrating layer 103 vs a non-metagrating layer. The emission intensities in the normal direction were determined using image analysis and used as the basis to overlay the two sets of characteristics for comparison. The degree of polarization is shown in the graph 701C as a function of wavelength. The degree of polarization for quasicrystal metagrating layers 103 is much less than for periodic square lattice metagrating.

[0017] In some embodiments, to improve upon the metagrating layer 103 applied to OLED 301 and other thin-film type displays, one or more microcavities may further be incorporated into the OLED display to enable more powerful control of the light emission characteristics of the display. Optical metamaterials are subwavelength components that are arranged in a specific pattern to create optical effects that cannot be achieved using conventional optics components. The addition of the metamaterial layer 103 inside an OLED device allows for light emission control that is especially attractive for increasing optics efficiency for near eye displays for augmented reality and virtual reality. These include control over the polarization of the emitted light, control of the angular emission cone, and control over the emission linewidth.

[0018] The addition of the metamaterial into the OLED changes the electromagnetic field formation inside of the OLED to enhance the light emission efficiency. The external quantum efficiency of OLEDs has greatly lagged behind the internal quantum efficiency which has reached nearly 100%. The reason for that disconnect is due to total internal reflection and

internal waveguide modes. A significant portion of the generated light in an OLED is lost due to coupling to internal waveguide modes because of the higher refractive index of the constituent layers of the OLED compared to air. The addition of metamaterial optics suppresses those waveguide losses and directs more light out the OLED. The difference in emission between an OLED 801 with the metamaterial versus an OLED 803 without the metamaterial as can be seen in FIG. 8.

[0019] In some embodiments, metamaterial layer 103 is placed underneath the emissive layers of the OLED. Typically, attempts to control the light emission of OLEDs has used transmissive metamaterials that manipulate the light as it passes through the metamaterials.

[0020] In contrast, the metamaterial layer 103 described herein works in the reflection mode and is composed of metallic plasmonic subwavelength components. The metamaterial layer 103 is fabricated before the deposition of the emissive layers which makes it compatible for top emitting OLEDs such as those found in micro displays. This makes it suitable for organic emissive layers found in OLEDs which are sensitive materials and thus are usually incompatible with additional lithography steps after the deposition of the organic layers. By controlling the enhanced emission of the OLED, the total light emission profile of the OLED can be modified.

[0021] In one embodiment, the metamaterial layer 103 leverages the physics of metamaterials and gratings to create the desired effect. The advantage of metagratings compared to other types of metamaterials is their lessened dependence on deeply subwavelength components. For metamaterials that operate in the visible spectrum, the proposed metagratings have minimum features sizes of greater than 100 nm compared to other optical metamaterials which may need feature sizes that are sub-100 nm. This results in the metagrating layer 103 being significantly easier to manufacture with standard photolithography techniques such as 193 nm deep ultraviolet (DUV) photolithography.

[0022] A proof of concept test device incorporating the above described metamaterial layer or metagrating is illustrated in FIG. 9. On the right is a conventional top emitting OLED 901, with a plurality of layers including an ultra-thin cathode layer 203, emission layer 204, and a reflector layer 205. A test device 903 is shown on the left and is substantially similar to the top emitting OLED 901 with the addition of a metamaterial layer 103 and the removal of the ultra-thin cathode layer 203.

[0023] The organic emitter in the test device 903 is 8-hydroxyquinolonato aluminum (Alq_3), a broad-band organic emitter which emits mostly in the green portion of the visible wavelength. For testing purposes, a set of test devices with the metamaterial layer 103 and a set of devices without the metamaterial layer 103 were created. The presence of the metamaterial was the only difference between the devices with both sets of devices being fabricated on the same substrate 207. Important to the performance of the metagrating layer 103 is the spacer thickness between the grating pattern itself and the backside metal reflector. The grating itself is formed from noble metals with good plasmonic properties in the visible wavelengths. Suitable metals include gold and silver. Other metals may be used. An example pattern 1001 for the metamaterial is shown in FIG. 10.

[0024] For purposes of testing, a 405 nm violet laser was used to induce fluorescence in the test devices and the emission was measured using a CCD camera. Narrow bandpass filters (FWHM = 10 nm) were used to evaluate the wavelength dependence of the emission. Devices with and without the inclusion of the metamaterial were imaged and analyzed. Results were averaged over multiple devices and hundreds of CCD camera images. The results of the test devices show that the inclusion of the metamaterial layer does change the emission profile. Emission in the forward direction is enhanced, as losses due to total internal reflection and waveguide modes are minimized.

[0025] Polarization dependence of these devices was also measured. The setup for the polarization dependent measurement is the same as above except for the presence of a linear polarizer placed between the filter and camera. This polarizer was rotated, and measurements were conducted. The 0-degree alignment was set where the emission enhancement was weakest and the other alignments (45-degrees and 90 degrees) of the linear polarizer was set with that as the reference.

[0026] The emissions with and without the metamaterials was compared using the following formula:

[0027] $$Improvement = \frac{Emission_{meta} - Emission_{nonmeta}}{Emission_{nonmeta}}$$

[0028] This formulation helps to show how much more light comes out of the metamaterial integrated devices compared to a reference device without a metamaterial enhancement. Different types of metamaterial patterns were used to create different emission effects.

[0029] FIG. 11 is an illustration of example graphs 1101 (e.g., the graphs 1101A and 1101B) showing improvements due to the metagrating layer 103. The graph 1101A shows the best forward emission enhancement measured was an improvement of 380%, which means 4.8x increase in light for a metamaterial integrated device compared to a reference device. This type of metamaterial pattern consists of a square lattice of circular plasmonic inserts. For this type of metamaterial pattern, there is a weak dependence on polarization. There is clearly a measured enhancement for all three alignments of the linear polarizer. The 0-degree alignment having the weakest enhancement, the 90-degree alignment having the strongest enhancement, and as expect, the 45-degree alignment having an enhancement in between the two. The polarization of the various alignments is illustrated in the graph 1101B.

[0030] For a line and space pattern metamaterial as shown in FIG. 10, the forward enhancement is not as strong as the square lattice metamaterial pattern, but the enhancement is more sensitive to polarization. As shown in 1101B, the highest measured improvement for the line and space pattern is 277% which corresponds to a 3.77x increase in light from the metamaterial enhanced device compared to a reference device with no metamaterial. Based on the results of the polarization measurements, the emission enhancement may be due completely to one polarization (90-degree alignment of the linear polarizer) with the other polarization (0-degree alignment) having no improvement and is in fact slightly suppressed. This means that the overall polarization distribution of the total emission goes from 1:1 for the reference device to something closer to 1:4 for the metamaterial integrated device.

[0031] Other types of metagrating patterns induce other effects. A 5-fold symmetric quasicrystal pattern of cylinders was also tested for the metagrating layer. This induced an enhancement of the emission across a broader range of wavelengths along with little dependence on polarization. Additional patterns such as randomly oriented cylinders, and other types of lattices such as triangle and hexagonal are all patterns of interest.

[0032] In some embodiments, the performance of the metamaterial enhanced OLED may be improved by integrating a planar microcavity. A planar microcavity structure for an OLED greatly enhances its forward emission intensity, as well as narrowing the emission linewidth. The combination of the microcavity along with the metamaterial layer greatly enhances the light emission control such as angular emission profile and emission linewidth.

[0033] Additionally, the metasurface layer 103 can be used to the tune the resonance of the microcavity. The resonance of the microcavity is important to determine the wavelength of the enhancement. Thus, different colors can be selected by an appropriate tuning of the resonance. Normally, the resonance of the microcavity is determined by the physical size of the cavity (total optical thickness). The total optical thickness includes the phase shift provided by

the metasurface which can be changed without altering the physical thickness of the metasurface or the entire cavity. However, the inclusion of a metamaterial layer 103 means that the cavity physical size can be fixed, while the metamaterial alters the resonance of the cavity by changing the total optical thickness. This means that microcavities with the same physical thickness can have differing resonances due to the presence of the designed metasurface within the cavity. Having a single physical thickness for the planar microcavity greatly increases its ease of fabrication, and thus the inclusion of the metamaterial layer to tune the resonance may greatly increase its commercial appeal.

[0034] FIG. 12 illustrates a combination of a metasurface layer 103 (e.g., metagrating) and a planar microcavity 1230. The planar microcavity 1230 is formed between two mirrors (e.g., a top dielectric mirror layer 1211 and back mirror layer 1209) with the metasurface layer 103 in between these mirrors. In one embodiment, the layers include a metal bottom mirror (e.g., back mirror layer 1209), a dielectric layer (e.g., SiO_2 layer 1207), a metasurface layer 103 (e.g., metagrating), additional transparent/semitransparent layers including the OLED active layers (e.g., organic layers 1203 and organic/inorganic layers 1205), a semitransparent contact electrode (e.g., semitransparent contact layer 1201), and a dielectric top mirror (e.g., top dielectric mirror layer 1211). Other layers may be supported.

[0035] The metasurface layer suppresses light emission in lateral directions if its dimensions are designed correctly. Without the microcavity, by itself, the metasurface layer enhances the forward emission of a range of wavelengths, whose emission along the plane of the layers is suppressed. Adding the microcavity provides spectral purity by allowing a narrow range of wavelengths to be emitted in the direction normal to the layers. At off-axis angles, there is a blue shift in the emission wavelength, a property characteristic of planar microcavities. Over a small range of solid angles, the emission will be spectrally narrow and is more intense than in a regular light emitter (without a metasurface or a microcavity). It will also be more

intense over a small range of wavelengths compared to a device without a microcavity (but with a metasurface).

[0036] The total optical thickness of the microcavity, L, is given by equation 1:

$$L(\lambda) \approx \frac{\lambda}{2}\left(\frac{n}{\Delta n}\right) + \sum_j n_j L_j + \left|\frac{\varphi_m}{4\pi}\lambda\right| + \phi_{mg} \qquad (1)$$

where $L(\lambda)$is the phase shift length provided by the metagrating, and: $\frac{\lambda}{2}\left(\frac{n}{\Delta n}\right)$ is the penetration depth of the wave into the dielectric mirror at wavelength λ. Δn is the difference in refractive index between the layers that constitute the dielectric mirror (exemplary materials are SiO_2 and Si_3N_4). n is the average index. The second term in equation 1 is the sum of the optical thickness (optical thickness = the product of physical thickness and refractive index) of all the layers between the mirrors except the metasurface. The third term in equation 1 is the penetration depth of the wave into the bottom mirror.

[0037] The phase shift in the metasurface layer 103 may be adjusted by altering the fraction of the two materials that constitute the metagrating/metasurface. For example, if the metagrating consists of Au and SiO_2, then increasing the fraction of Au without changing the period will change the phase shift and hence the total optical thickness of the cavity. This method offers a way to change the cavity resonance wavelength without changing the physical thickness of any of the layers. This is a big advantage over prior art solutions for changing the emission wavelength or color of a device.

[0038] To change the emission wavelength normal to the device the dimensions of the metagrating layer 103 may be changed as described below. The period of the metagrating layer 103 defines which wavelength range is suppressed along waveguide directions (these same wavelengths are preferentially emitted in the forward direction). When the period of the

metagrating layer 103 is changed, the phase length of the metagrating layer 103 must be changed so that the designed wavelength coincides with the cavity resonance of the microcavity, favoring microcavity enhancement.

[0039] The cavity modes of the microcavity are given by equation 2:

$$m\lambda = 2L(\lambda) \quad (2)$$

where m is the mode index and λ is the wavelength and $L(\lambda)$is given by equation 1.

[0040] Another way to change L is to change the optical thickness of one or more layers of the microcavity. However, the combination of optical thickness changes by phase changes in the metagrating and layer composition/thickness changes has not been contemplated.

[0041] To change the optical thickness, either the physical cavity length can be varied or the phase shift can be manipulate using the metagrating. The optical thickness determines cavity resonance mode, which will enhance the emission of one narrow set of wavelengths while suppressing other wavelengths. This will be used select the color.

[0042] A white OLED is composed of multiple emission layers of differing colors that create an overall white emission. By integrating the metagrating later 103 and planar microcavity structure into this white OLED, the emission color of the OLED can be varied between red, green, and blue. The color emission is dependent on the optical thickness of the microcavity, which is controlled by the physical length of the microcavity and the phase shift provided by the metagrating.

[0043] Overall, the structure formed by the metasurface and microcavity described herein are designed to result in effective mode confinement in the lateral (in-plane) direction due to refractive index modulation. To achieve this two additional structures are described. A first structure 1300 shown in FIG. 13 includes a metasurface layer and a vertical planar

microcavity 1230 and has light emission through the transparent substrate. A second structure 1400 shown in FIG. 14 includes light emission from the top and includes a metasurface with defects and a vertical microcavity 1230.

[0044] In both these structures, photons are confined in a smaller area compared to the charge injection area. This happens because of photon redistribution in accordance with the periodic metagrating structure in which "defects" are included. The higher refractive index in the defect areas will lead to a concentration of photons in such areas, much like in a photonic crystal structure with a defect. From the perspective of etendue, the more photons are concentrated within the device, the lower will be the expected etendue. In particular, both structures have a significantly high ratio between the area of charge injection (which is uniform across large areas) and the effective areas from which the photons are emitted. Furthermore, both structures present a planar interface to the organic layers and will potentially have the same reliability of existing micro-OLEDs.

[0045] The first structure 1300 of FIG. 13 is a dielectric quarter wave stack with reflectivity of about 80-90% formed on a transparent substrate such as glass. The first structurer 1300 includes a cathode layer 203, an electron injection layer 1301, an electron transport layer 1303, an emission layer 204, a hole transport layer 1305, a hole injection layer 1307, an ITO semitransparent layer 1309, a metasurface layer 103, and a transparent substrate layer 207.

[0046] Exemplary materials for the stack are SiO_2 and Si_3N_4, which have a high enough refractive index contrast to be suitable. A dielectric mirror constitutes the bottom mirror of the planar microcavity. An additional layer of SiO_2 (about 100 nm thick) is deposited above the stack. This is followed by a lithography step (e-beam or advanced optical lithography) in which the high-resolution pattern in the photoresist is transferred to the SiO_2 by etching at ~ 50-100 nm.

[0047] Gold or silver (50-100 nm thick) is then deposited and a lift-off process removes the resist with the metal in select areas leaving behind embedded metal with the same pattern

as the resist pattern (shown in FIG. 13). The process is designed so that the top surface of the metal is ideally aligned with the surface of the remaining SiO_2 such that an almost planar surface results. This facilitates deposition of the device layers beginning with indium tin oxide (by sputtering). The hole injection and transport layers are then deposited followed by the emission layer (doped) and electron transport layers as described in the materials section. The cathode consisting of 2 nm of Ca and thick Al is then deposited to complete the device. The cathode acts as the top reflector in the planar microcavity 1230.

[0048] The first structure 1300 of FIG. 13 may have the following optical features. Excitons are formed uniformly across the structure, as the structure is homogeneous from an electrical standpoint. Excitons do not diffuse very far (about 5 nm) and photon generation is also expected to be uniform. However, the lateral refractive index profile will result in a concentration of the photons in the "defect" regions which have no metal (and therefore a higher n value).

[0049] Optically the structure functions as a concentrator in which photons generated uniformly across the structure are concentrated and emitted from a much smaller area corresponding to the high index defect regions. Detailed COMSOL simulations may be performed to optimize the photon emission zone to keep it small in area relative to the overall structure. This will result in an array of photon emission areas. The vertical microcavity (consisting of the top Al mirror – the cathode and the bottom dielectric mirror) will result in outcoupling of the photons in a narrow emission cone. The lateral index profile will also result in suppression of emission in the in-plane directions. The combined effect of the metasurface and the microcavity of the structure will result in a narrow far field emission. Since the defects are separated by about a micron (greater than the wavelength), they can be regarded as isolated emitters from an optical standpoint and the etendue of such structures will be small, enabling higher intensities after focusing than is possible from a uniform planar emitter. The high ratio of

electrically active area (the entire device) and the effective emission area (the defect areas) will also be advantageous for small etendue. Finally, emission takes place through the metagrating, which will result in some absorption losses. However, the defect areas (which have no metal) from which photon emission primarily takes place, will result in less absorption loss and more efficient light emission from the proposed structure.

[0050] The second structure 1400 of FIG. 14 is substantially similar to the structure described and shown in FIG. 12 with the addition of defects in the metasurface layer 103. A defect is a region of the metasurface layer with no metal resulting in a higher refractive index than other non-defect regions of the metasurface layer 103.

[0051] Although exemplary implementations may refer to utilizing aspects of the presently disclosed subject matter in the context of one or more stand-alone computer systems, the subject matter is not so limited, but rather may be implemented in connection with any computing environment, such as a network or distributed computing environment. Still further, aspects of the presently disclosed subject matter may be implemented in or across a plurality of processing chips or devices, and storage may similarly be effected across a plurality of devices. Such devices might include personal computers, network servers, and handheld devices, for example.

[0052] Although the subject matter has been described in language specific to structural features and/or methodological acts, it is to be understood that the subject matter defined in the appended claims is not necessarily limited to the specific features or acts described above. Rather, the specific features and acts described above are disclosed as example forms of implementing the claims.

What is claimed:

1. A display comprising:

a first device layer;

a second device layer; and

a reflecting metasurface, wherein the reflecting metasurface is applied between the first device layer and the second device layer.

2. The display of claim 1, wherein the display is an organic light emitting device (OLED) display.

3. The display of claim 1, wherein the metasurface is a one-dimensional pattern.

4. The display of claim 1, wherein the metasurface is a two-dimensional pattern.

5. The display of claim 1, wherein the reflecting metasurface comprises a first material and a second material.

6. The display of claim 5, wherein the first material is gold and the second material has a refractive index of at least 1.5.

7. The display of claim 5, wherein the first material and the second material are patterned into sub-wavelength patterns.

8. The display of claim 5, wherein the first material and the second material are lattices.

9. The display of claim 8, wherein the lattices comprise square lattices, triangular lattices, 1-dimensional gratings, and quasicrystal patterns.

10. A display comprising:

a first device layer;

a second device layer;

a microcavity; and

a metamaterial layer, wherein the metamaterial layer is applied between the first device layer and the second device layer and the microcavity is between the metamaterial layer and the second device layer.

11. The display of claim 10, wherein the first device layer is an emissive layer.

12. The display of claim 11, wherein the metamaterial layer is applied to the display before the emissive layer.

13. The display of claim 10, wherein the metamaterial comprises a metallic plasmonic subwavelength material.

14. The display of claim 10, wherein the display is an organic light emitting device (OLED) display.

15. The display of claim 10, wherein the metamaterial layer comprises a metagrating.

16. The display of claim 15, wherein the metagrating has a minimum feature size that is greater than 100 nm.

17. The display of claim 10, wherein the metagrating is manufactured using photolithography.

18. The display of claim 10, wherein the metagrating is manufactured using 193 nm deep photolithography.

19. The display of claim 10, wherein the microcavity is a planar microcavity.

20. The display of claim 10, wherein the display is incorporated into an augmented reality or virtual reality headset.

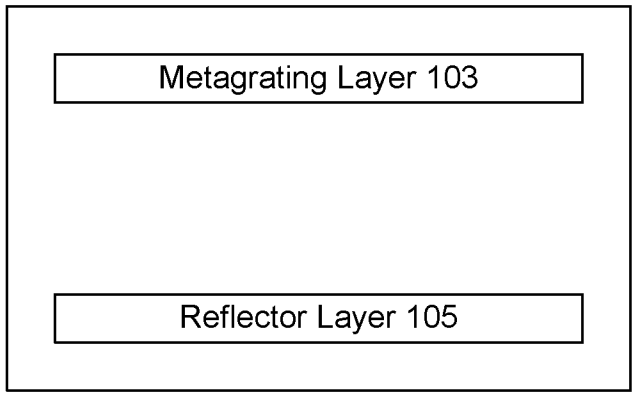

101

FIG. 1

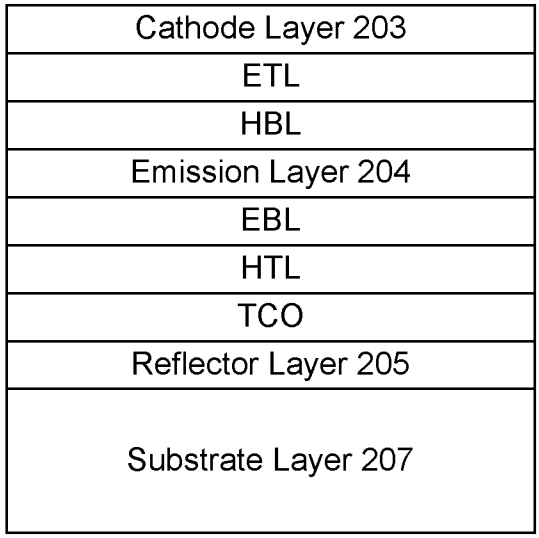
Cathode Layer 203
ETL
HBL
Emission Layer 204
EBL
HTL
TCO
Reflector Layer 205
Substrate Layer 207
201

FIG. 2

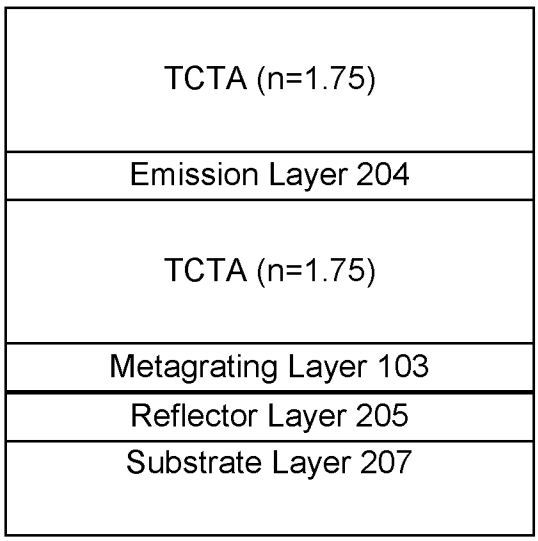
TCTA (n=1.75)
Emission Layer 204
TCTA (n=1.75)
Metagrating Layer 103
Reflector Layer 205
Substrate Layer 207

301

FIG. 3

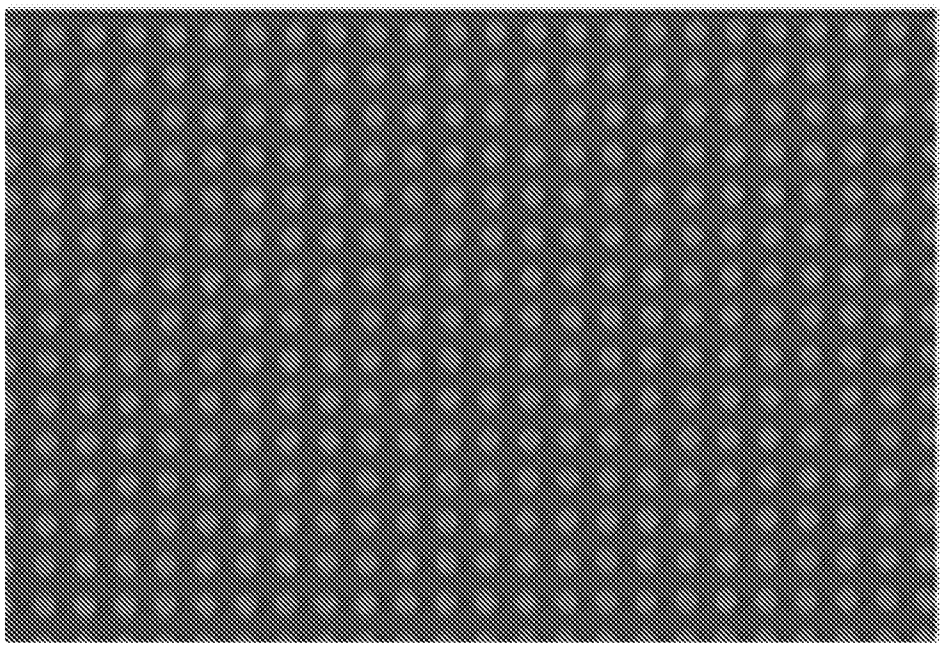

401

FIG. 4

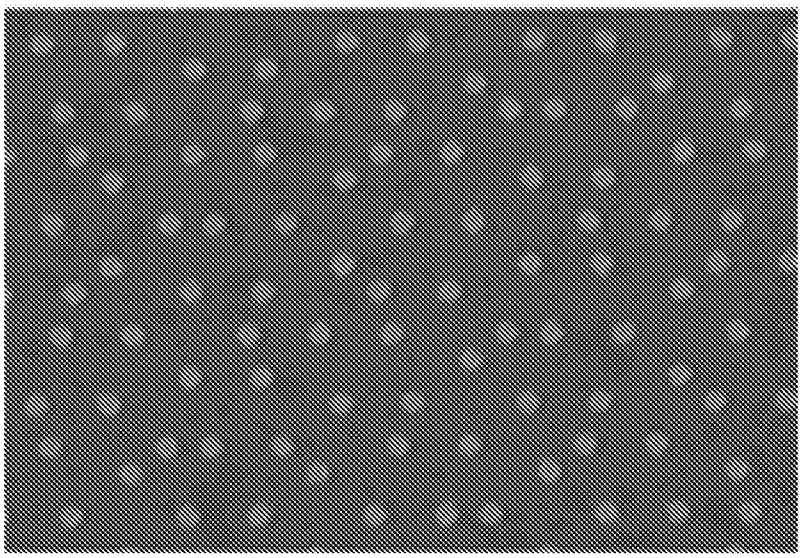

501

FIG. 5

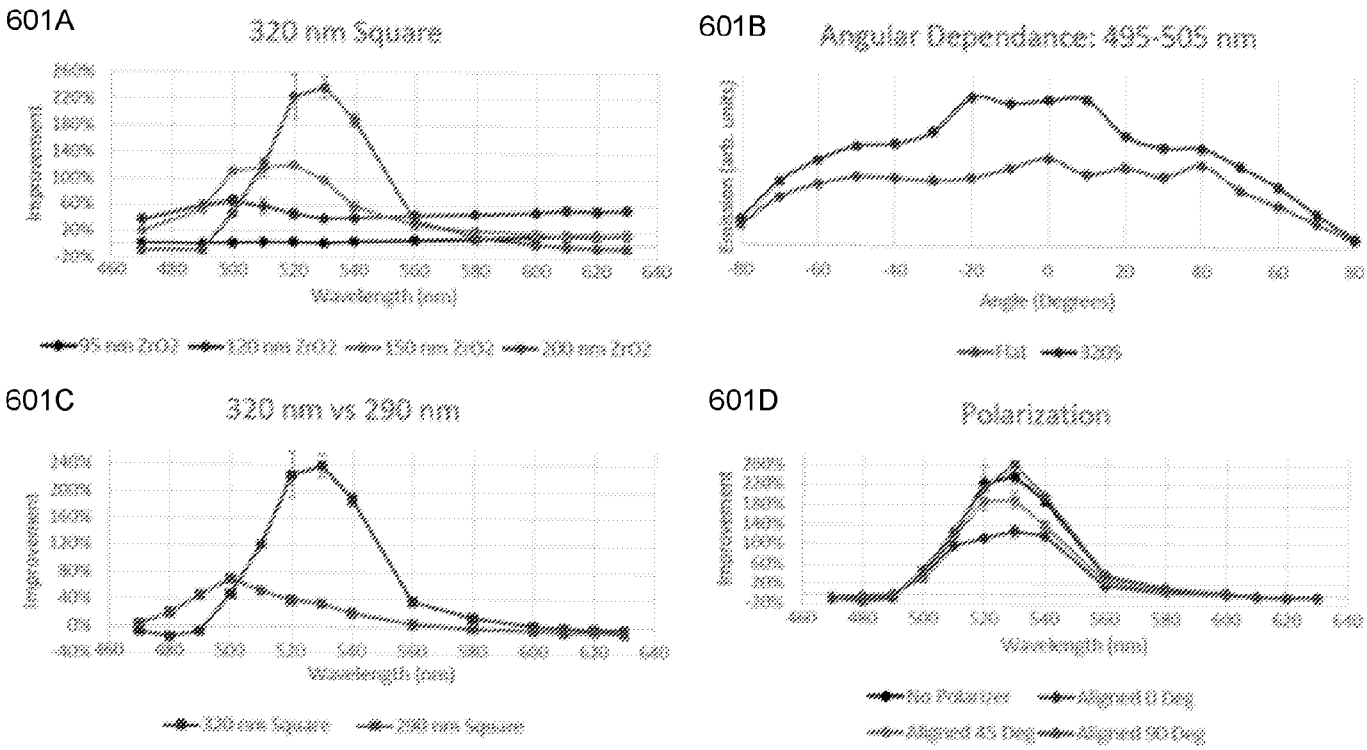
601A
320 nm Square
Wavelength (nm)
601B
Angular Dependance: 495-505 nm
Angle (Degrees)
601C
320 nm vs 290 nm
Wavelength (nm)
601D
Polarization
Wavelength (nm)

FIG. 6

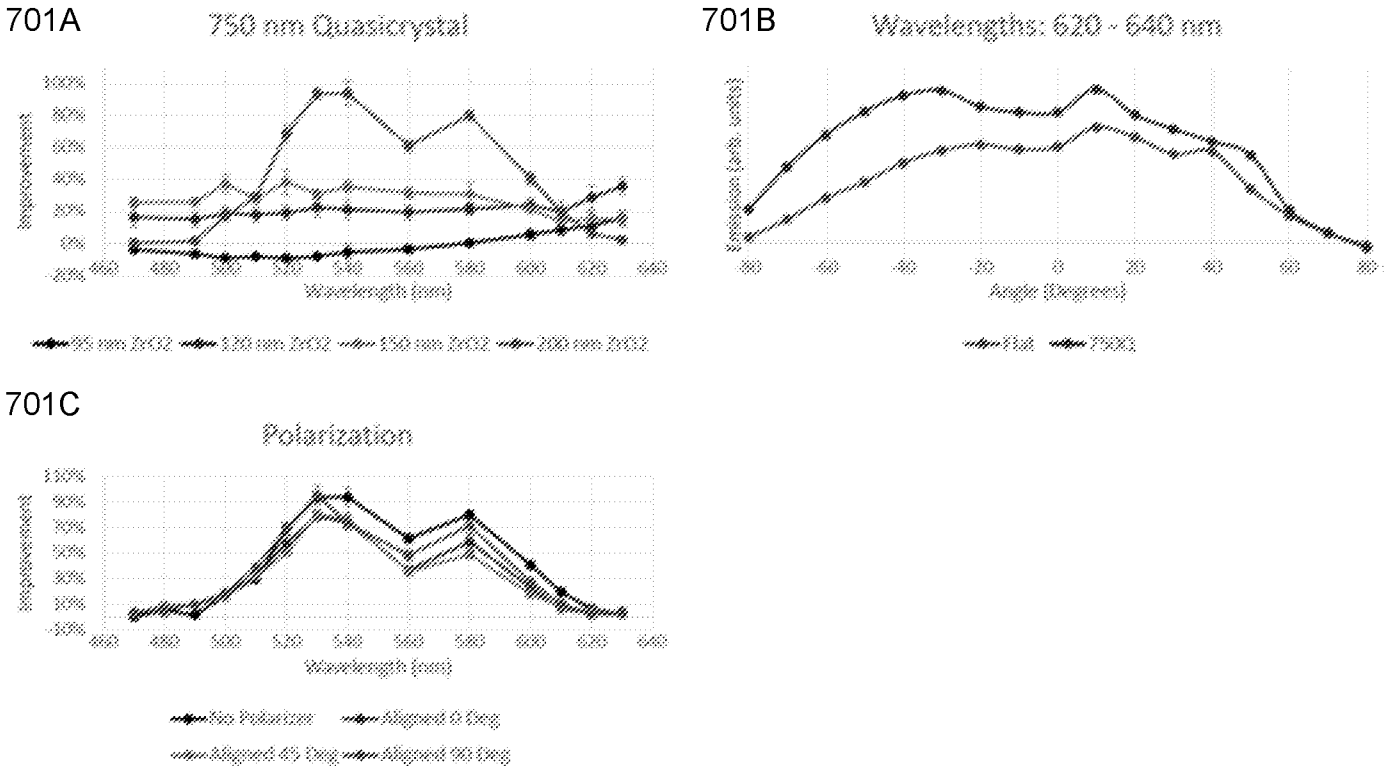
701A
750 nm Quasicrystal
Wavelength (nm)
701B
Wavelengths: 620 - 640 nm
Angle (Degrees)
701C
Polarization
Wavelength (nm)

FIG. 7

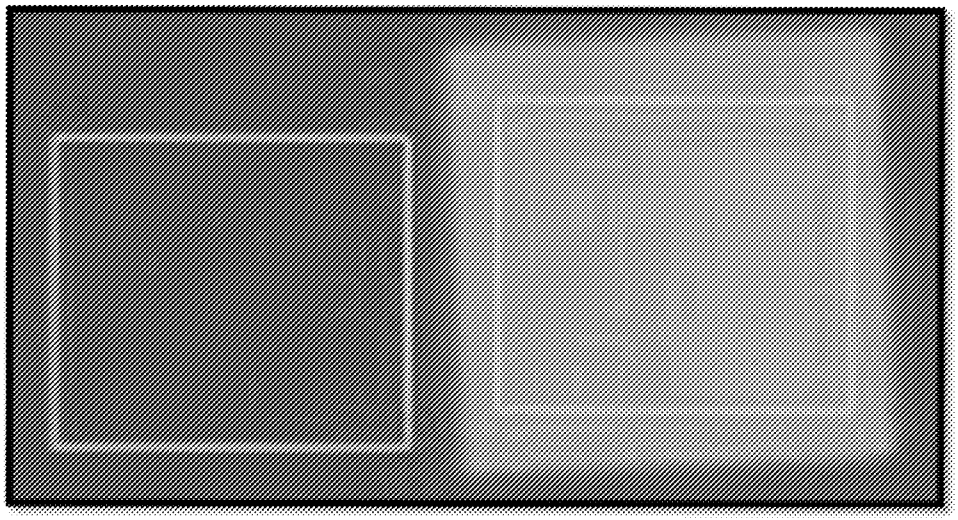

FIG. 8

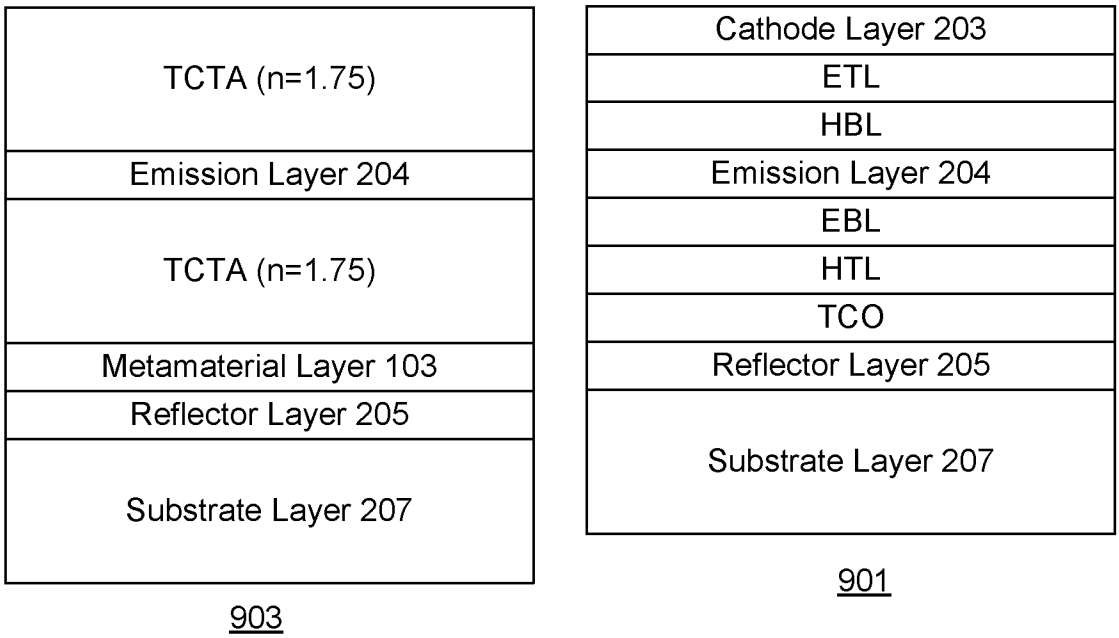
TCTA (n=1.75)
Emission Layer 204
TCTA (n=1.75)
Metamaterial Layer 103
Reflector Layer 205
Substrate Layer 207
903
Cathode Layer 203
ETL
HBL
Emission Layer 204
EBL
HTL
TCO
Reflector Layer 205
Substrate Layer 207
901

FIG. 9

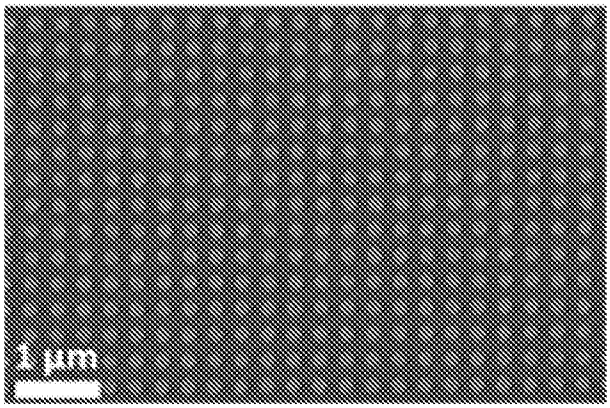

1001

FIG. 10

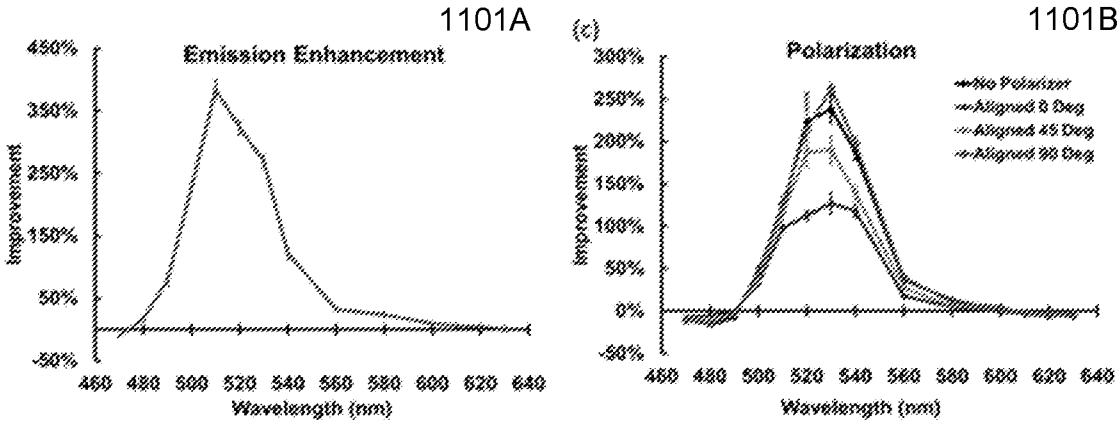
1101A
Emission Enhancement
450%
350%
250%
150%
50%
-50%
Improvement
460 480 500 520 540 560 580 600 620 640
Wavelength (nm)
(c)
1101B
Polarization
300%
250%
200%
150%
100%
50%
0%
-50%
Improvement
No Polarizer
Aligned 0 Deg
Aligned 45 Deg
Aligned 90 Deg
460 480 500 520 540 560 580 600 620 640
Wavelength (nm)

FIG. 11

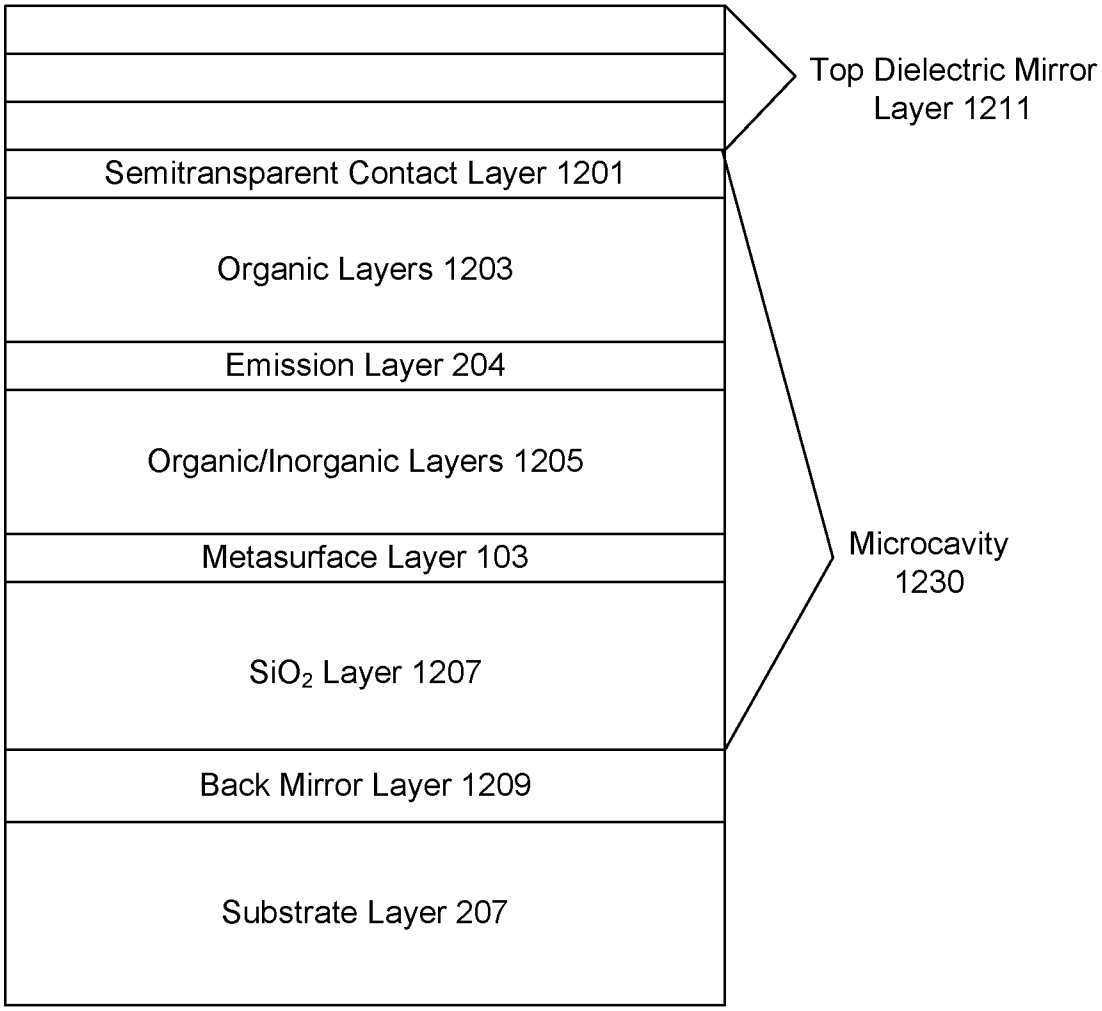
Top Dielectric Mirror Layer 1211
Semitransparent Contact Layer 1201
Organic Layers 1203
Emission Layer 204
Organic/Inorganic Layers 1205
Metasurface Layer 103
SiO_2 Layer 1207
Microcavity 1230
Back Mirror Layer 1209
Substrate Layer 207

FIG. 12

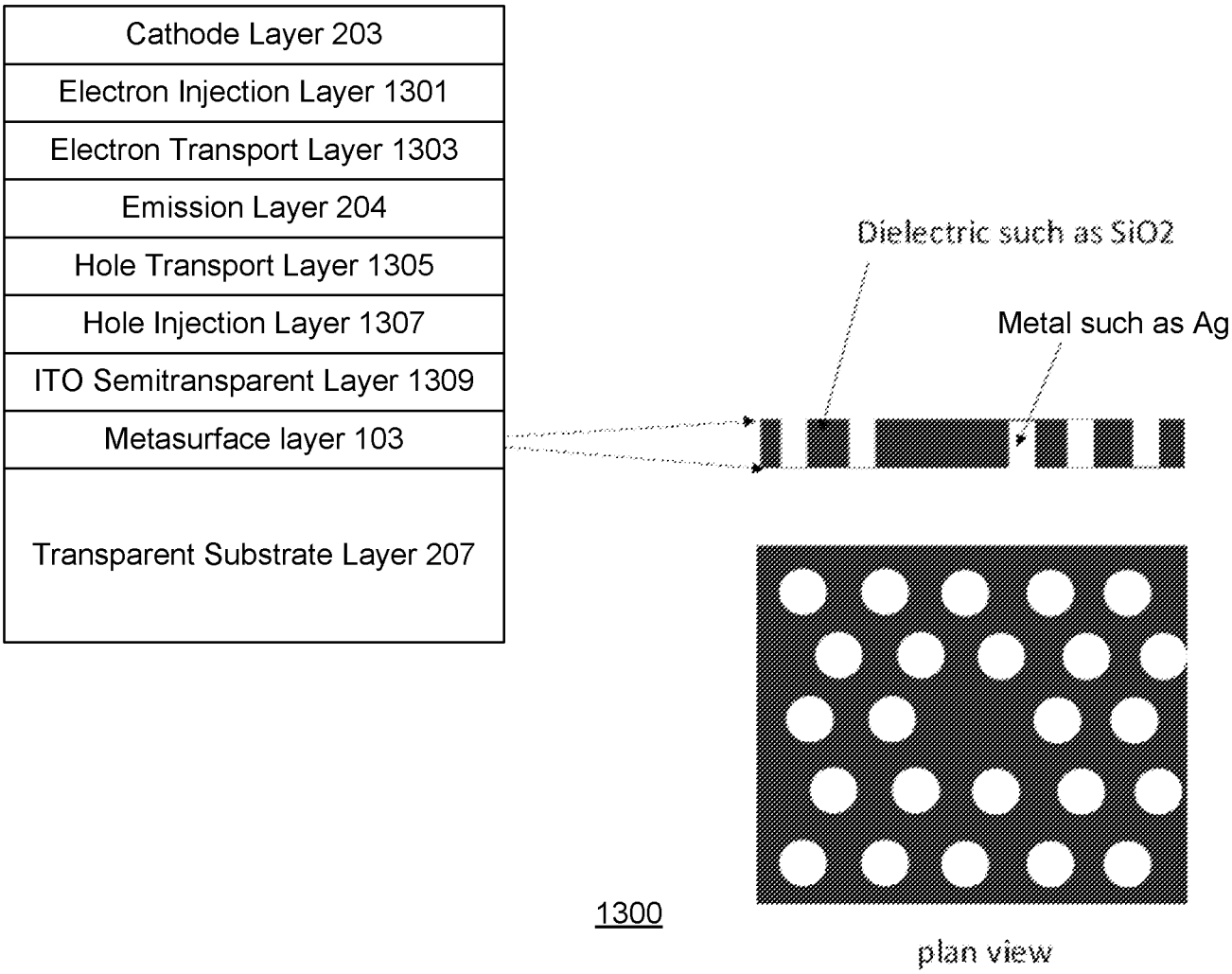
Cathode Layer 203
Electron Injection Layer 1301
Electron Transport Layer 1303
Emission Layer 204
Hole Transport Layer 1305
Hole Injection Layer 1307
ITO Semitransparent Layer 1309
Metasurface layer 103
Transparent Substrate Layer 207
Dielectric such as SiO2
Metal such as Ag
1300
plan view

FIG.13

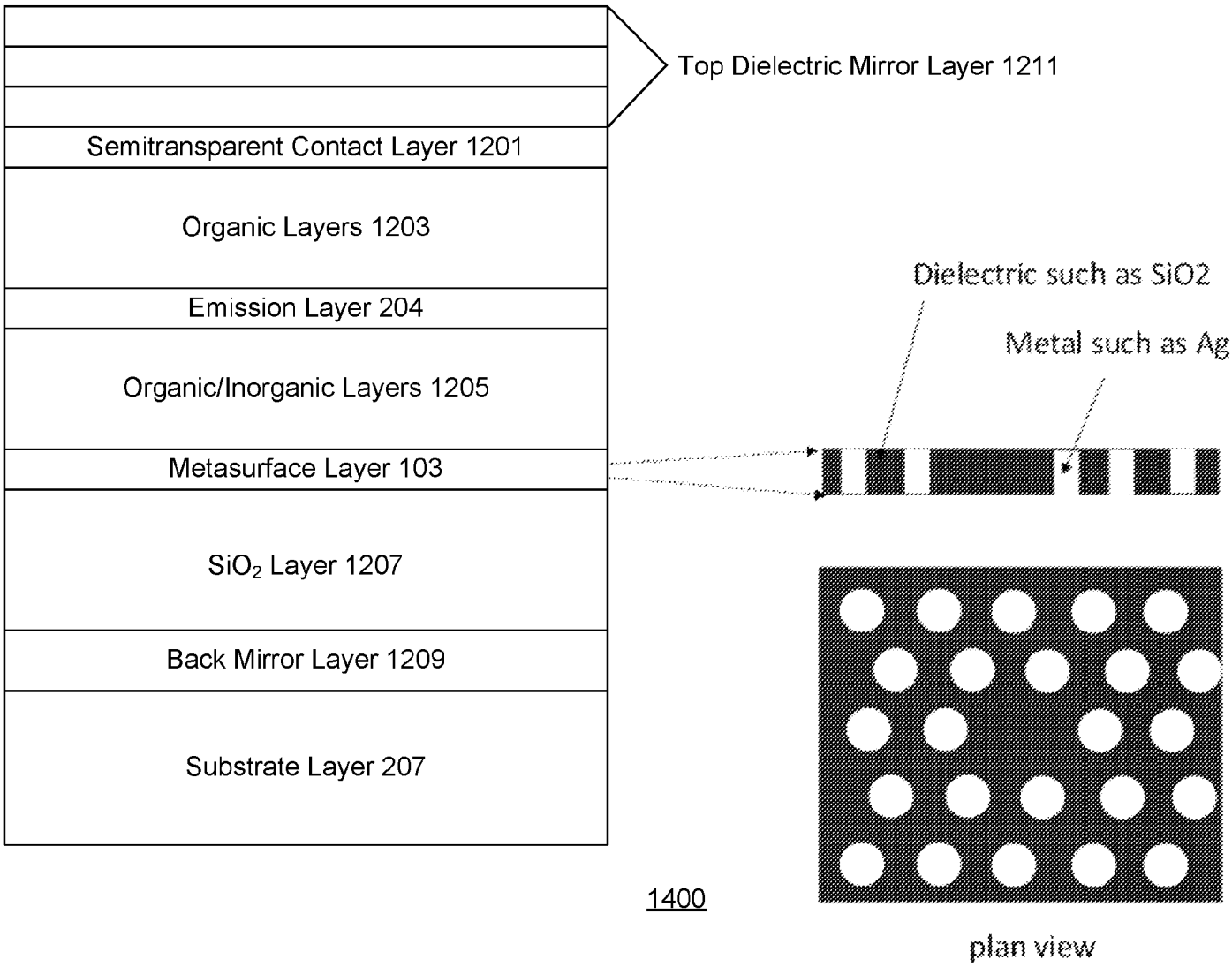
Top Dielectric Mirror Layer 1211
Semitransparent Contact Layer 1201
Organic Layers 1203
Emission Layer 204
Organic/Inorganic Layers 1205
Metasurface Layer 103
SiO_2 Layer 1207
Back Mirror Layer 1209
Substrate Layer 207
Dielectric such as SiO2
Metal such as Ag
1400
plan view

FIG. 14

INTERNATIONAL SEARCH REPORT

International application No.
PCT/US2021/046622

A. CLASSIFICATION OF SUBJECT MATTER

IPC(8) - H05B 33/14; G02B 1/00; G02B 5/00; G02B 5/18; G02B 5/30; G02B 27/00; G02B 27/28 (2021.01)
CPC - H05B 33/14; G02B 1/00; G02B 5/18; G02B 5/30; G02B 27/28; H05B 33/00; H05B 33/12; H05B 33/20 (2021.08)

According to International Patent Classification (IPC) or to both national classification and IPC

B. FIELDS SEARCHED

Minimum documentation searched (classification system followed by classification symbols)
see Search History document

Documentation searched other than minimum documentation to the extent that such documents are included in the fields searched
see Search History document

Electronic data base consulted during the international search (name of data base and, where practicable, search terms used)
see Search History document

C. DOCUMENTS CONSIDERED TO BE RELEVANT

Category*	Citation of document, with indication, where appropriate, of the relevant passages	Relevant to claim No.
X --- Y	US 2017/0133631 A1 (UNIVERSAL DISPLAY CORPORATION) 11 May 2017 (11.05.2017) entire document	1-9 --- 10-20
Y	US 2020/0243800 A1 (SAMSUNG ELECTRONICS CO. LTD.) 30 July 2020 (30.07.2020) entire document	10-20

☐ Further documents are listed in the continuation of Box C. ☐ See patent family annex.

* Special categories of cited documents:
"A" document defining the general state of the art which is not considered to be of particular relevance
"D" document cited by the applicant in the international application
"E" earlier application or patent but published on or after the international filing date
"L" document which may throw doubts on priority claim(s) or which is cited to establish the publication date of another citation or other special reason (as specified)
"O" document referring to an oral disclosure, use, exhibition or other means
"P" document published prior to the international filing date but later than the priority date claimed
"T" later document published after the international filing date or priority date and not in conflict with the application but cited to understand the principle or theory underlying the invention
"X" document of particular relevance; the claimed invention cannot be considered novel or cannot be considered to involve an inventive step when the document is taken alone
"Y" document of particular relevance; the claimed invention cannot be considered to involve an inventive step when the document is combined with one or more other such documents, such combination being obvious to a person skilled in the art
"&" document member of the same patent family

Date of the actual completion of the international search	Date of mailing of the international search report
27 October 2021	DEC 01 2021
Name and mailing address of the ISA/US Mail Stop PCT, Attn: ISA/US, Commissioner for Patents P.O. Box 1450, Alexandria, VA 22313-1450 Facsimile No. 571-273-8300	Authorized officer Harry Kim Telephone No. PCT Helpdesk: 571-272-4300